Six transformations in one pot …

… allow the stereoselective synthesis of various di- and trisubstituted vinyl triflones, and several heteroaryl triflones from *gem*-dibromovinyl substrates. In their Communication on page 12628 ff., N. Shibata et al. explore the key steps of this procedure. The cover picture shows a “Japanese-style painting” by Mami Shibata (a Tama Art University student), named “Kaze” (“breeze” in English). The six transformations in one pot proceed very smoothly, like birds in a breeze.

Molecular Electronics

In their Communication on page 12536 ff., K. Müllen, L. F. Chi, et al. report uniform monolayer to hexalayer dendritic organic semiconductor microstripes grown at monolayer precision.

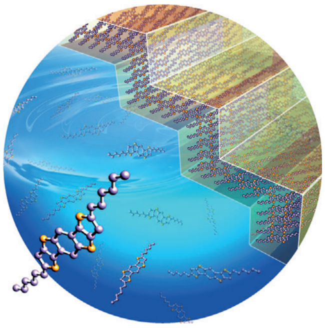

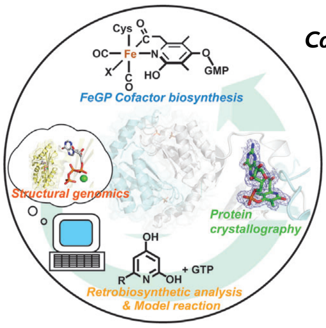

Cofactor Biosynthesis

In their Communication on page 12555 ff., S. Sima et al. elucidate one reaction step of the biosynthesis of [Fe]-hydrogenase-cofactor, with the help of a structural genomics approach, model reactions, and X-ray crystallography.

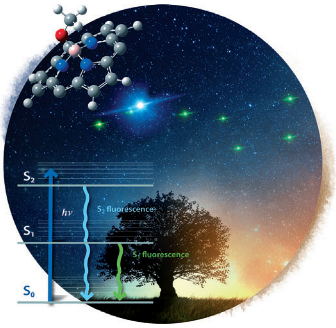

Subporphyrins

In their Communication on page 12632 ff., A. Osuka, D. Kim et al. describe the S_2 fluorescence and the photophysical behavior of the higher excited states of subporphyrins.

How to contact us:

Editorial Office:
E-mail: angewandte@wiley-vch.de
Fax: (+49) 6201–606-331
Telephone: (+49) 6201–606-315

Reprints, E-Prints, Posters, Calendars:
Carmen Leitner
E-mail: chem-reprints@wiley-vch.de
Fax: (+49) 6201–606-331
Telephone: (+49) 6201–606-327

Copyright Permission:
Bettina Loycke
E-mail: rights-and-licences@wiley-vch.de
Fax: (+49) 6201–606-332
Telephone: (+49) 6201–606-280

Online Open:
Margitta Schmitt, Carmen Leitner
E-mail: angewandte@wiley-vch.de
Fax: (+49) 6201–606-331
Telephone: (+49) 6201–606-315

Subscriptions:
www.wileycustomerhelp.com
Fax: (+49) 6201–606-184
Telephone: 0800 1800536 (Germany only)
+44(0) 1865476721 (all other countries)

Advertising:
Marion Schulz
E-mail: mschulz@wiley-vch.de
jspiess@wiley-vch.de
Fax: (+49) 6201–606-550
Telephone: (+49) 6201–606-565

Courier Services:
Boschstrasse 12, 69469 Weinheim

Regular Mail:
Postfach 101161, 69451 Weinheim

Angewandte Chemie International Edition is a journal of the Gesellschaft Deutscher Chemiker (GDCh), the largest chemistry-related scientific society in continental Europe. Information on the various activities and services of the GDCh, for example, cheaper subscription to *Angewandte Chemie International Edition*, as well as applications for membership can be found at **www.gdch.de** or can be requested from GDCh, Postfach 900440, D-60444 Frankfurt am Main, Germany.

GDCh
GESELLSCHAFT
DEUTSCHER CHEMIKER

Service

Spotlight on Angewandte's Sister Journals *12476 – 12479*

Author Profile

"My favorite saying is "yes, we can!"
I can never resist travelling to new places ..."
This and more about Marina A. Petrukhina can be found on page 12480.

Marina A. Petrukhina **12480**

News


K. Al-Shamery


P. Bäuerle


S. Hell


P. R. Schreiner


C. Wöll


H. Cölfen


F. H. Schacher


P. Schwille


P. H. Seeberger


H.-J. Freund

New Members of the Deutsche Akademie der Naturforscher Leopoldina and the Berlin–Brandenburg Academy of Sciences and Humanities Academy **12481**

Prize of the Berlin–Brandenburg Academy of Sciences and Humanities: H. Cölfen **12481**

Dr. Hermann Schnell Fellowship: F. H. Schacher **12482**

Obituaries

Manfred Schlosser disappeared on June 26, 2013, shortly after his 79th birthday, in the Swiss mountains. His contributions to the scientific community include not only many valuable new methods but also new insight that provides a mechanistic basis for the rational description of organometallic reactivity.

Manfred Schlosser (1934–2013)

F. Leroux* ______ **12483**

Books

Bioinspiration and Biomimicry in Chemistry

Gerhard F. Swiegers

reviewed by Z. Schnepp ______ **12484**

Highlights

Cellular Transport

K. Bacia* ______ **12486 – 12488**

Intracellular Transport Mechanisms: Nobel Prize for Medicine 2013

How are biomolecules transported between cellular compartments? James E. Rothman, Randy W. Schekman, and Thomas C. Südhof made seminal contributions to answering this question with their research into the molecular mechanism of intracellular vesicle transport. For their achievements, the researchers were awarded the Nobel Prize in Physiology or Medicine on October 7, 2013.

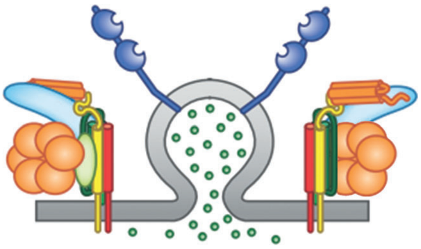

Computational Chemistry

G. Groenhof* ______ **12489 – 12491**

Solving Chemical Problems with a Mixture of Quantum-Mechanical and Molecular Mechanics Calculations: Nobel Prize in Chemistry 2013

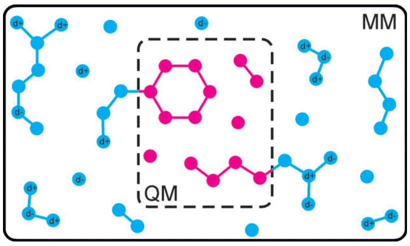

The significance of computer simulations in such varied fields as chemistry, biophysics, structural biology, and materials science is emphasized by the award of the Nobel Prize in Chemistry 2013 to three of the most important pioneers of computational chemistry. Computer simulations are widely used today to interpret experimental results, to test hypotheses, and as inspiration for experiments.

For the USA and Canada: ANGEWANDTE CHEMIE International Edition (ISSN 1433-7851) is published weekly by Wiley-VCH, PO Box 191161, 69451 Weinheim, Germany. Air freight and mailing in the USA by Publications Expediting Inc., 200 Meacham Ave., Elmont, NY 11003. Periodicals postage paid at Jamaica, NY 11431. US POSTMASTER: send address changes to *Angewandte Chemie*, Journal Customer Services, John Wiley & Sons Inc., 350 Main St., Malden, MA 02148-5020. Annual subscription price for institutions: US$ 11.738/10.206 (valid for print and electronic / print or electronic delivery); for individuals who are personal members of a national chemical society prices are available on request. Postage and handling charges included. All prices are subject to local VAT/sales tax.

Essays

Homogenous Catalysis

W. Keim* 12492 – 12496

Oligomerization of Ethylene to α-Olefins: Discovery and Development of the Shell Higher Olefin Process (SHOP)

Luck, talent, and hard work: Currently, over a million tons of α-olefins are manufactured per annum using the Shell Higher Olefin Process (SHOP). The discovery of the process was the result of correct model conceptions and lucky coincidence. W. Keim, one of the main participants in the development of SHOP, gives a personal account of the events.

Minireviews

Nucleic Acid Modifications

M. Winnacker, E. T. Kool* 12498 – 12508

Artificial Genetic Sets Composed of Size-Expanded Base Pairs

Expanded horizons: Stretched nucleobases, which are larger than the bases of the natural Watson–Crick architecture, lead to the development of artificial genetic sets. These systems have properties that are useful for understanding fundamental biochemical questions as well as for the development of new biotechnological, biomedical, and nanostructural tools and methods.

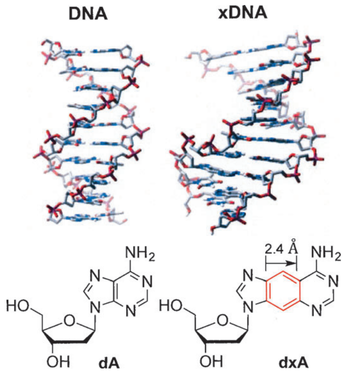

Reviews

Redox-Active Ligands

A. I. O. Suarez, V. Lyaskovskyy,
J. N. H. Reek, J. I. van der Vlugt,
B. de Bruin* 12510 – 12529

Complexes with Nitrogen-Centered Radical Ligands: Classification, Spectroscopic Features, Reactivity, and Catalytic Applications

Radical character is found in many complexes with nitrogen ligands, as shown by studies of their electronic structure, spectroscopic features, and (catalytic) reactivity. The Review focuses on the reactivity of detectable aminyl ($[M(^{\bullet}NR_2)]$), nitrene/imidyl ($[M(^{\bullet}NR)]$), and nitridyl radical complexes ($[M(^{\bullet}N)]$), and their application in the (catalytic) synthesis of nitrogen-containing organic molecules such as aziridines and amines.

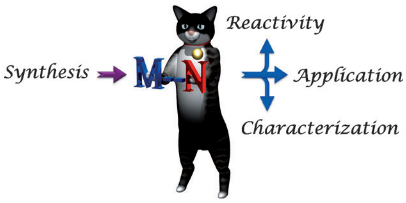

Communications

Molecular Electronics

L. Q. Li, P. Gao, W. C. Wang, K. Müllen,*
H. Fuchs, L. F. Chi* 12530 – 12535

Growth of Ultrathin Organic Semiconductor Microstripes with Thickness Control in the Monolayer Precision

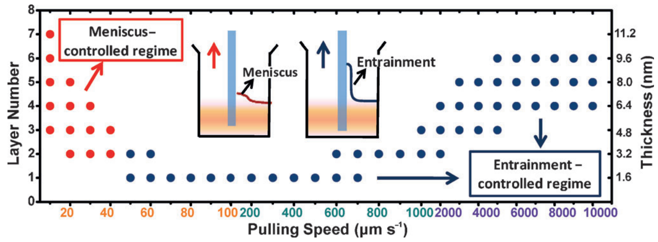

Organic semiconductors: Growth of ultrathin (< 15 nm), continuous, and microstructured organic semiconductor (OSC) films at monolayer precision is important for organic electronics and a challenging task. Uniform monolayer to hexalayer (ca. 1.6–12 nm; see picture) dendritic OSC microstripes at monolayer precision are grown by a dip-coating process.

Frontispiece

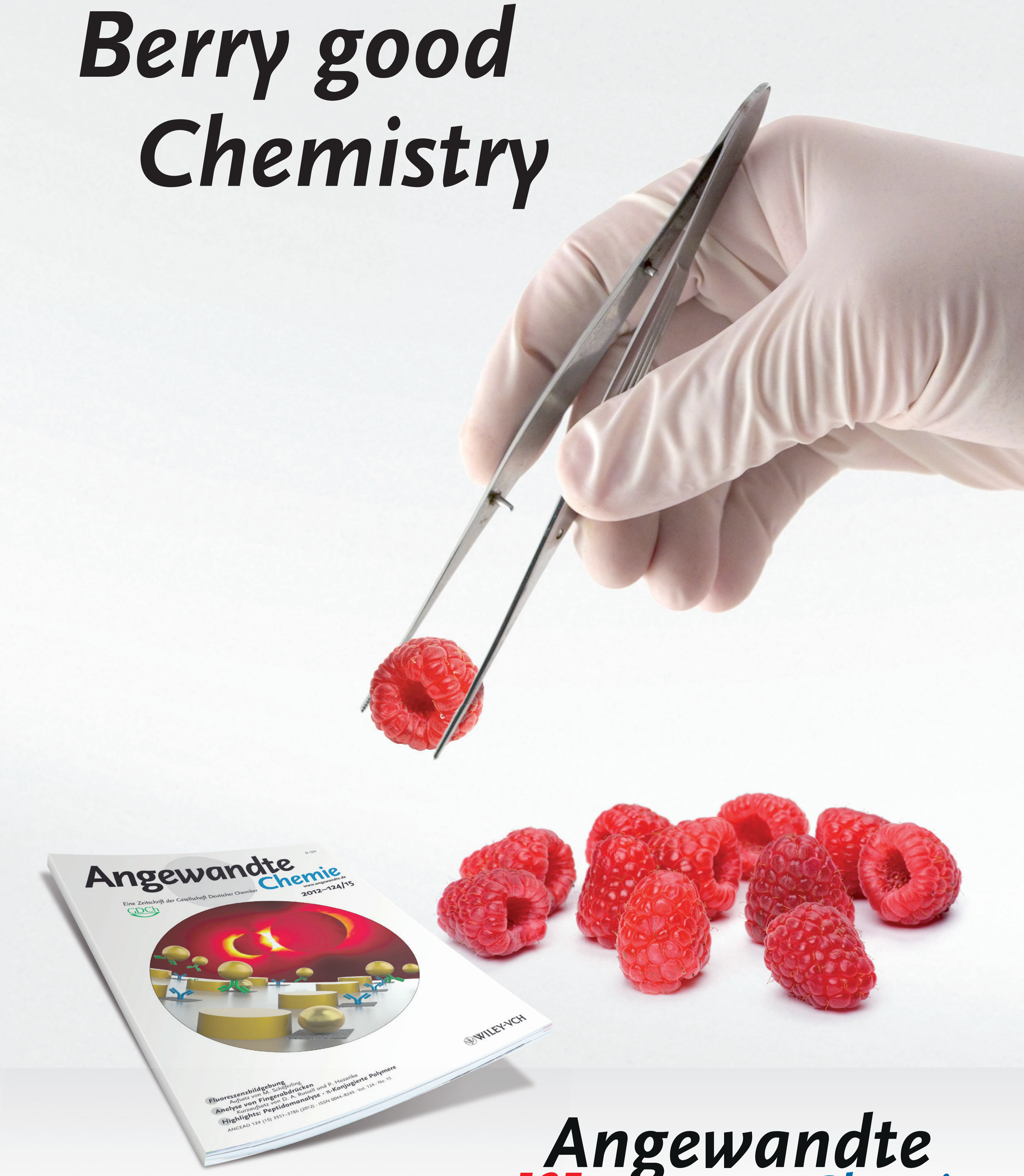
Berry good
Chemistry
Angewandte Chemie
Eine Zeitschrift der Gesellschaft Deutscher Chemiker
2012–124/15
WILEY-VCH
Fluoreszenzbildgebung
Aufsatz von M. Schäferling
Analyse von Fingerabdrücken
Kurzaufsatz von D. A. Russell und P. Hazarika
Highlights: Peptidomanalyse · π-Konjugierte Polymere
ANCEAD 124 (15) 3551–3786 (2012) · ISSN 0044-8249 · Vol. 124 · No. 15

Copolymerization

D. Takeuchi,* Y. Chiba, S. Takano,
K. Osakada* ________ 12536 – 12540

Double-Decker-Type Dinuclear Nickel Catalyst for Olefin Polymerization: Efficient Incorporation of Functional Co-monomers

Inside Cover

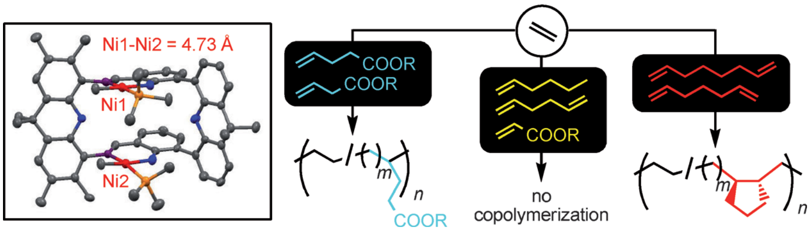

A dinuclear Ni complex with a double-decker structure (see scheme) and a short Ni–Ni distance promotes the copolymerization of ethylene with functional monomers. Matching of the Ni–Ni distance with the co-monomer structure resulted in polymers containing a high density of the co-monomer unit.

Lithium-Ion Batteries

S. Afyon, M. Wörle,
R. Nesper* ________ 12541 – 12544

A Lithium-Rich Compound Li$_7$Mn(BO$_3$)$_3$ Containing Mn^{2+} in Tetrahedral Coordination: A Cathode Candidate for Lithium-Ion Batteries

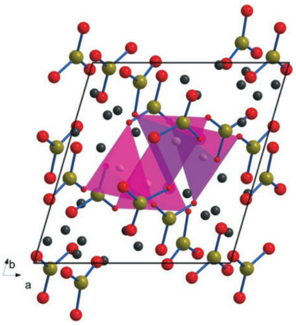

Filled to capacity: Li$_7$Mn(BO$_3$)$_3$ is lithium-rich and fulfills the prerequisites for a high-capacity cathode for Li-ion batteries. It contains a framework of MnO$_4$ tetrahedra (pink) and BO$_3^{3-}$ ions (B green, O red, Li black). By employing a nano-composite to enhance electronic conductivity, a first charge capacity of 280 mAh g^{-1}, and a specific energy of 1135 Wh kg^{-1} are obtained within 4.7–1.7 V at a rate of 10 mA g^{-1}.

Contact Electrification

Z.-H. Lin, G. Cheng, L. Lin, S. Lee,
Z. L. Wang* ________ 12545 – 12549

Water–Solid Surface Contact Electrification and its Use for Harvesting Liquid-Wave Energy

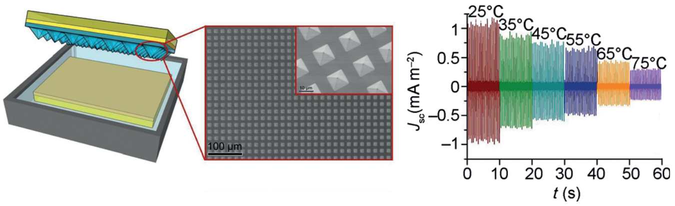

Electrical wave mechanics: A newly designed triboelectric nanogenerator is based on the contact electrification between a patterned polydimethylsiloxane pyramid array and water. Cost-effective and simple, the prototype triboelectric nanogenerator shows the potential to harvest energy from liquid waves and serve as chemical and temperature sensors.

Self-Assembly

Y. Hisamatsu, S. Banerjee, M. B. Avinash,
T. Govindaraju,
C. Schmuck* ________ 12550 – 12554

A Supramolecular Gel from a Quadruple Zwitterion that Responds to Both Acid and Base

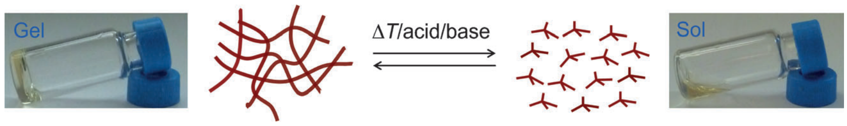

Four arms: A quadruple zwitterion based on a pentaerythritol core forms thermoreversible gels in DMSO driven by the formation of ion-paired dimers between the zwitterionic units. Furthermore, it exhibits reversible gel–sol transitions in response to both acid and base.

Cofactor Biosynthesis

T. Fujishiro, H. Tamura, M. Schick,
J. Kahnt, X. Xie, U. Ermler,
S. Shima* ________ **12555 – 12558**

Identification of the HcgB Enzyme in [Fe]-Hydrogenase-Cofactor Biosynthesis

Inside Back Cover

[Fe]-Hydrogenase requires the iron guanylylpyridinol (FeGP) cofactor for activity. The function of HcgB, an enzyme in the biosynthesis of the FeGP cofactor, was predicted by structural genomics and confirmed by model reactions and various analytical methods: HcgB catalyzes the terminal guanylyltransferase reaction for the formation of guanylylpyridinol. GMP = guanosine monophosphate.

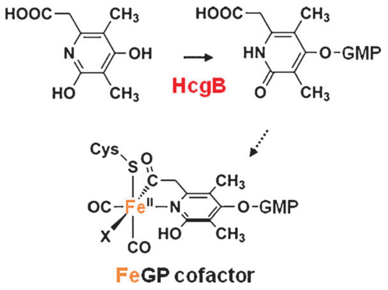

Synthetic Methods

M. Szostak,* B. Sautier, M. Spain,
M. Behlendorf,
D. J. Procter* ________ **12559 – 12563**

Selective Reduction of Barbituric Acids Using SmI_2/H_2O: Synthesis, Reactivity, and Structural Analysis of Tetrahedral Adducts

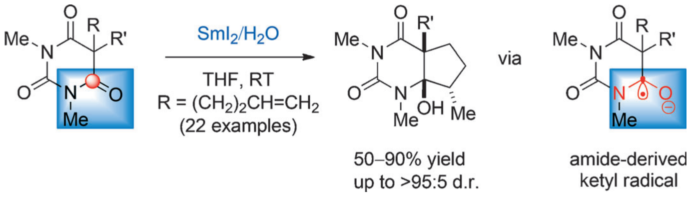

Making a mark: Since the 1864 landmark discovery by Adolf von Baeyer, barbituric acids have played a prominent role in organic synthesis. Herein, the first chemoselective monoreduction of barbituric acids to the corresponding hemiaminals is described. The method delivers mono- and bicyclic hemiaminal products by a general single-electron-transfer polarity reversal mechanism.

Helical Structures

M. Lee, J. Shim, P. Kang, I. A. Guzei,
S. H. Choi* ________ **12564 – 12567**

Structural Characterization of α/β-Peptides having Alternating Residues: X-ray Structures of the 11/9-Helix from Crystals of Racemic Mixtures

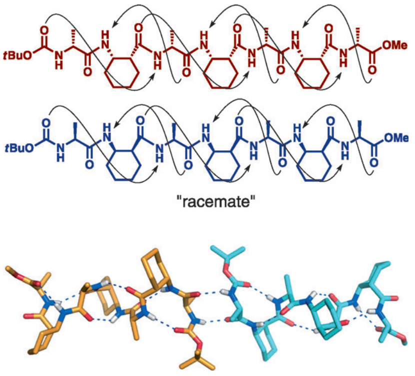

Twisted (crystal)sisters: The structures of the α/β-peptide 11/9-helix were determined by single-crystal X-ray crystallography. The racemic compounds adopt centrosymmetric crystal packing, and display fully folded 11/9-helical conformations. The helical parameters of the 11/9-helix are analogous to those of the 3_{10}-helix, despite different hydrogen-bonding types.

Pigment Discoloration

W. Anaf, K. Janssens,
K. De Wael* ________ **12568 – 12571**

Formation of Metallic Mercury During Photodegradation/Photodarkening of α-HgS: Electrochemical Evidence

The red pigment α-HgS tends to blacken in the presence of light and chloride ions. Hypotheses exist for the decomposition and discoloration, including formation of β-HgS (black) or of metallic mercury, but these have not been detected on naturally or synthetically degraded HgS paint. Electrochemical experiments now demonstrate the formation of metallic mercury in the presence of light and chloride ions.

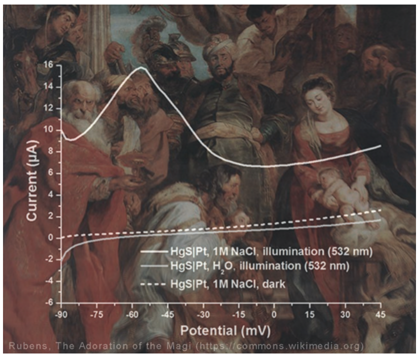

Rubens, The Adoration of the Magi (https://commons.wikimedia.org)

Got it PEGged: PEGylation and zwitterionization have distinct effects on the pharmacokinetic and tumor-targeting properties of luminescent gold nanoparticles (AuNPs), although both strategies lead to effective renal clearance. High tumor-targeting efficiency and specificity were obtained with PEGylated AuNPs, whereas rapid tumor detection was more readily achieved with zwitterionic AuNPs. HD = hydrodynamic diameter, GS = glutathione.

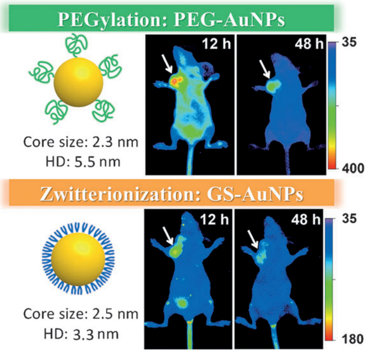

Imaging Agents

J. Liu, M. Yu, X. Ning, C. Zhou, S. Yang, J. Zheng* ________ **12572 – 12576**

PEGylation and Zwitterionization: Pros and Cons in the Renal Clearance and Tumor Targeting of Near-IR-Emitting Gold Nanoparticles

---

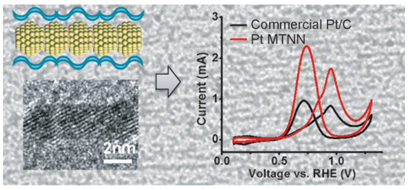

Structure-enhanced catalytic activity: An ultrathin platinum multiple-twinned nanowire network is shown to be an efficient electrocatalyst (see picture). This material has a higher electrochemical surface area and exhibits a much improved activity toward both the oxygen reduction reaction and the methanol oxidation reaction relative to commercial Pt/C catalysts.

Electrocatalysis

L. Ruan, E. Zhu, Y. Chen, Z. Lin, X. Huang, X. Duan, Y. Huang* ________ **12577 – 12581**

Biomimetic Synthesis of an Ultrathin Platinum Nanowire Network with a High Twin Density for Enhanced Electrocatalytic Activity and Durability

---

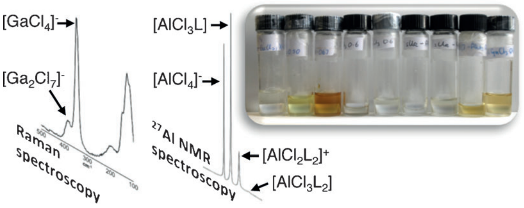

Confused complexes: Reaction of a range of donor molecules with $AlCl_3$ or $GaCl_3$, gives mobile liquids with very high metal contents. They contain statistically distributed mixtures of anionic, cationic, and neutral complexes in equilibrium. These liquid coordination complexes (LCCs), have high conductivity, tunable Lewis acidity, and low vapor pressure.

Liquid Coordination Complexes

F. Coleman, G. Srinivasan, M. Swadźba-Kwaśny* ________ **12582 – 12586**

Liquid Coordination Complexes Formed by the Heterolytic Cleavage of Metal Halides

---

Kinetics determined by NMR: Whereas most measurements of kinetic parameters of a ligand–protein complex use displacement of the ligand, protein displacement can give accurate off-rates in solution (see picture). Analytical and simulation results are given for the apparent off-rate obtained by protein displacement.

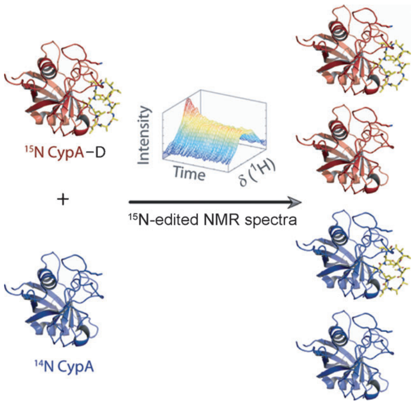

Ligand–Protein Complexes

H. Launay, B. Parent, A. Page, X. Hanoulle,* G. Lippens* ________ **12587 – 12591**

Dissociation Kinetics of a Binary Complex in Solution by Protein Displacement

Bioconjugation

N. Toda, S. Asano,
C. F. Barbas, III* ———— **12592 – 12596**

Rapid, Stable, Chemoselective Labeling of Thiols with Julia–Kocieński-like Reagents: A Serum-Stable Alternative to Maleimide-Based Protein Conjugation

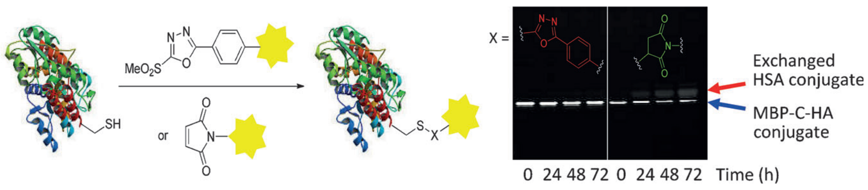

Exquisite chemoselectivity for cysteine has been found for methylsulfonylphenyloxadiazole compounds under various buffer conditions. Furthermore, the resulting protein conjugates have superior stability to cysteine–maleimide conjugates in human plasma (HSA = human serum albumin, MBP-C-HA = maltose-binding protein). This new thiol-click reaction offers a new approach to generate stable protein conjugates and Pegylated proteins.

G-Quadruplexes

B. G. Rusu, F. Cunin,
M. Barboiu* ———— **12597 – 12601**

Real-Time Optical Detection of Stabilized Artificial G-Quadruplexes Under Confined Conditions

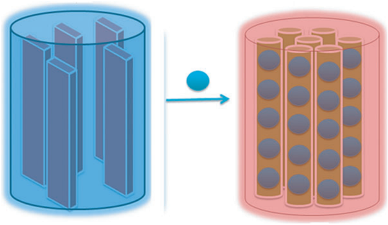

The color of self-assembly: Porous silicon (pSi) can be used as a scaffolding matrix to stabilize G-quadruplexes under confined conditions. When G-quadruplexes were infused into the pores, a change in the film color was observed, so that confinement and stabilization of the G-quadruplexes can be easily observed.

Rotational Dynamics

Q.-C. Zhang, F.-T. Wu, H.-M. Hao, H. Xu, H.-X. Zhao,* L.-S. Long,* R.-B. Huang, L.-S. Zheng ———— **12602 – 12605**

Modulating the Rotation of a Molecular Rotor through Hydrogen-Bonding Interactions between the Rotator and Stator

Two molecular rotors were synthesized (see picture). An investigation of the rotator rotation based on the imaginary parts of the complex dielectric constant (ε'') for each molecular rotor at various frequencies and temperatures revealed that the rotation of the mono-component molecular rotor could be modulated through hydrogen-bonding interactions between the rotator and the stator.

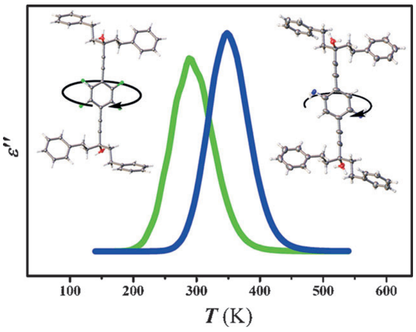

Mesoporous Materials

D. Chandra, K. Saito, T. Yui,
M. Yagi* ———— **12606 – 12609**

Crystallization of Tungsten Trioxide Having Small Mesopores: Highly Efficient Photoanode for Visible-Light-Driven Water Oxidation

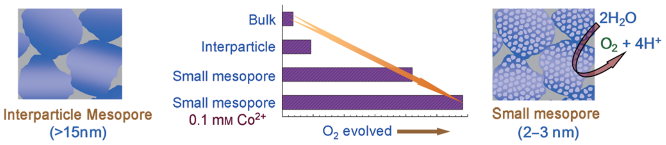

Small mesopores are more efficient: A mesoprous oxide semiconductor (tungsten trioxide) having small mesopores was crystallized at high temperature (550 °C) by a simple one-step procedure. The highly crystalline mesoporous WO_3 has an extremely high surface area which improves the visible-light-driven photoelectrochemical performance of water oxidation (see picture) relative to WO_3 having interparticle mesopores.

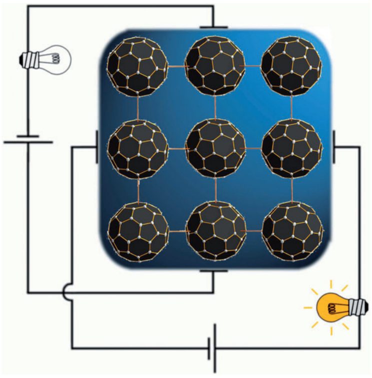

Spin and charge transport: The electronic and structural properties obtained from $KC_{60}(THF)_5{\cdot}2\,THF$ single crystals are reported (see picture). An important finding is the presence of one-dimensional electric conductivity and the observation of counterintuitive anisotropy for electron transport.

Fullerides

A. Kromer, U. Wedig, E. Roduner,
M. Jansen,
K. Y. Amsharov* ———— **12610 – 12614**

Counterintuitive Anisotropy of Electron Transport Properties in $KC_{60}(THF)_5{\cdot}2\,THF$ Fulleride

---

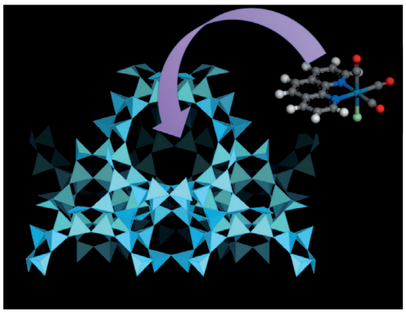

Whodunit? $[Re(phen)(CO)_3Cl]$ (phen = 1,10-phenanthroline) has been entrapped within a faujasite zeolite. For this material, changes in the photoluminescence intensity, wavelength, and lifetime are observed upon exposure to solvent vapors. Every solvent vapor produces a unique combination of photophysical parameters that can be used as a fingerprint of the vapor.

Vapor Sensing

A. Saha, Z. Panos, T. Hanna, K. Huang,
M. Hernández-Rivera,
A. A. Martí* ———— **12615 – 12618**

Three-Dimensional Solvent-Vapor Map Generated by Supramolecular Metal-Complex Entrapment

---

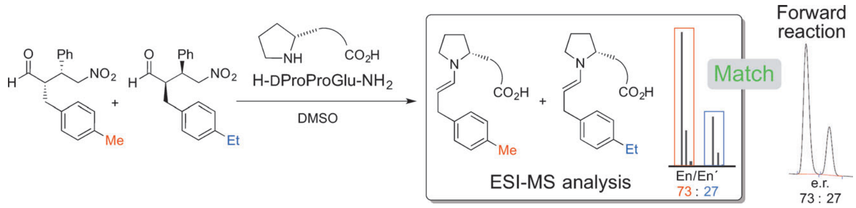

Looking back: The asymmetric organocatalytic 1,4-addition of aldehydes to nitroolefins was studied by ESI-MS. Analysis of the back reaction starting from quasienantiomeric mass-labeled 1,4-adducts (see scheme) provided conclusive evidence for an enamine rather than an enol mechanism, and allowed identification of the enantioselectivity-determining step.

Asymmetric Catalysis

F. Bächle, J. Duschmalé, C. Ebner,
A. Pfaltz,*
H. Wennemers* ———— **12619 – 12623**

Organocatalytic Asymmetric Conjugate Addition of Aldehydes to Nitroolefins: Identification of Catalytic Intermediates and the Stereoselectivity-Determining Step by ESI-MS

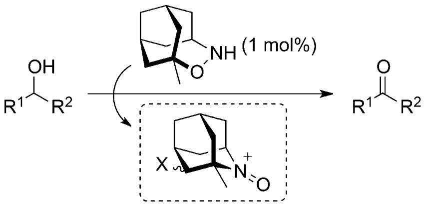

Strong, silent type: A novel alkoxyamine-type organocatalyst has been discovered for alcohol oxidation (see scheme). The alkoxyamine exhibits a high catalytic activity for the oxidation of alcohols to afford the corresponding carbonyl compounds in high yield by oxidative transformation into an oxoammonium ion, which is proposed to serve as an active species.

Synthetic Methods

Y. Sasano, K. Murakami, T. Nishiyama,
E. Kwon, Y. Iwabuchi* —— **12624 – 12627**

3-Methyl-4-oxa-5-azahomoadamantane: Alkoxyamine-Type Organocatalyst for Alcohol Oxidation

Synthetic Methods

X.-H. Xu, M. Taniguchi, X. Wang,
E. Tokunaga, T. Ozawa, H. Masuda,
N. Shibata* ———— **12628 – 12631**

Stereoselective Synthesis of Vinyl Triflones and Heteroaryl Triflones through Anionic $\mathrm{O}\rightarrow\mathrm{C_{vinyl}}$ and $\mathrm{N}\rightarrow\mathrm{C_{vinyl}}$ Trifluoromethanesulfonyl Migration Reactions

Front Cover

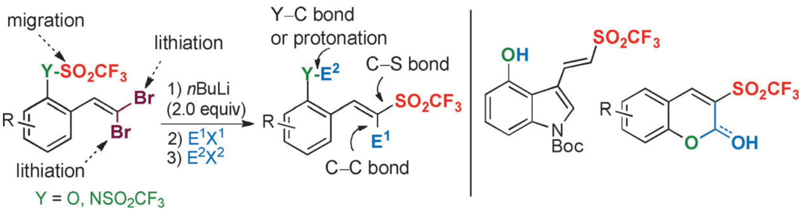

Six transformations, one pot: Various di- and trisubstituted vinyl triflones, as well as several heteroaryl triflones, were stereoselectively synthesized from easily accessible *gem*-dibromovinyl substrates (see scheme, Boc = *tert*-butoxycarbonyl). The highlights of this synthetic method lie in the remote $\mathrm{O}\rightarrow\mathrm{C_{vinyl}}$ or $\mathrm{N}\rightarrow\mathrm{C_{vinyl}}$ triflyl migrations and the one-pot, three-step protocol.

Subporphyrins

J. Sung, P. Kim, S. Saga, S. Hayashi,
A. Osuka,* D. Kim* ——— **12632 – 12635**

S_2 Fluorescence Dynamics of *meso*-Aryl-Substituted Subporphyrins

Back Cover

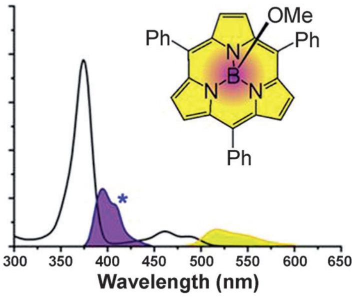

S_2 Fluorescence: Subporphyrins are intriguing compounds, but the behavior of their higher excited states has not been studied thus far. The S_2 fluorescence of subporphyrins has now been investigated; internal conversion from the S_2 to the S_1 state was revealed to occur within approximately 300 fs. The two transition dipole moments of the degenerate S_2 states are orthogonally oriented despite the C_3 symmetry of the subporphyrin.

Photochemistry

Y. Li, H. Ji, C. Chen,* W. Ma,
J. Zhao ———— **12636 – 12640**

Concerted Two-Electron Transfer and High Selectivity of TiO_2 in Photocatalyzed Deoxygenation of Epoxides

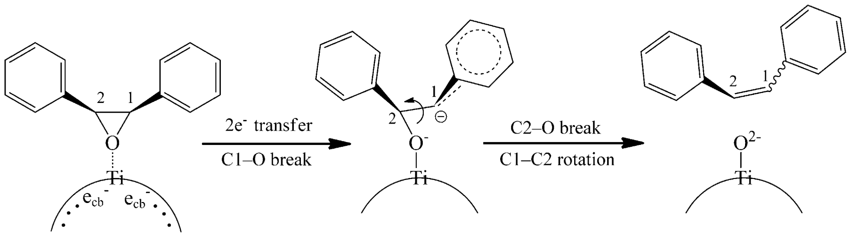

No two ways about it: In the photocatalytic deoxygenation of epoxides, the TiO_2 particle concertedly transfers two stored electrons to generate a carbanion intermediate, which dissociates to the alkene product. This pathway ensures the higher alkene and stereoselectivity of the photocatalytic deoxygenation than those involving a single-electron transfer.

Asymmetric Catalysis

H. Guo,* H. Liu, F.-L. Zhu, R. Na, H. Jiang,
Y. Wu, L. Zhang, Z. Li, H. Yu, B. Wang,
Y. Xiao, X.-P. Hu,*
M. Wang ———— **12641 – 12645**

Enantioselective Copper-Catalyzed [3+3] Cycloaddition of Azomethine Ylides with Azomethine Imines

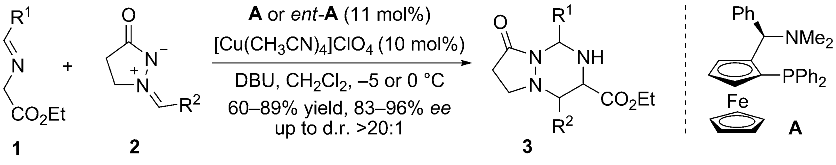

The more dipoles, the merrier: An asymmetric [3+3] cycloaddition of azomethine ylides derived from imines **1** with azomethine imines **2** in the presence of a chiral ferrocenylphosphine–copper catalyst afforded highly functionalized heterocyclic products **3** in high yield with excellent enantio- and diastereoselectivity (see scheme; DBU = 1,8-diazabicyclo[5.4.0]undec-7-ene). The 1,3-dipolar reaction partners can be readily prepared from aldehydes.

Uranium Siloxides

C. Camp, C. E. Kefalidis, J. Pécaut,
L. Maron, M. Mazzanti* **12646 – 12650**

Controlled Thermolysis of Uranium (Alkoxy)siloxy Complexes: A Route to Polymetallic Complexes of Low-Valent Uranium

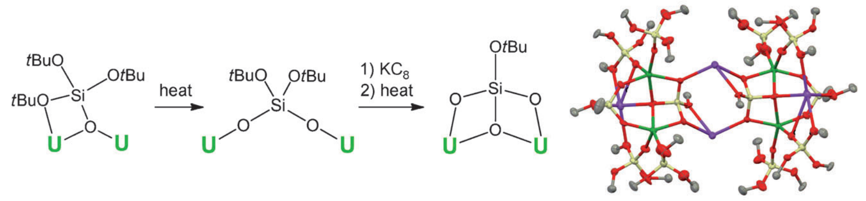

Decomposition into higher species: Intramolecular U^{III}-mediated homolytic C–O bond cleavage in U^{III} (alkoxy)siloxy complexes at low temperature and subsequent reduction with KC_8 led to unprecedented polymetallic complexes containing siloxy, silanediolate, and silanetriolate ligands (see example: U green, Si yellow, K blue, O red). Such compounds may be useful precursors to uranium ceramics relevant for catalysis and the storage of spent nuclear fuel.

Synthetic Methods

M. M. D. Wilde,
M. Gravel* **12651 – 12654**

Bis(amino)cyclopropenylidenes as Organocatalysts for Acyl Anion and Extended Umpolung Reactions

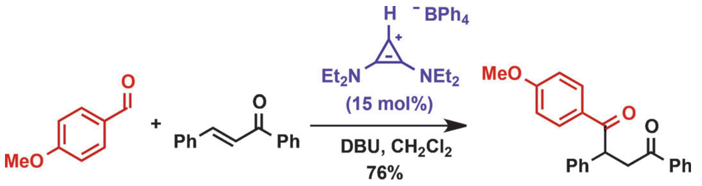

Back to BACs: In the pursuit of novel carbene organocatalysts, bis(amino)cyclopropenylidenes (BACs) were explored as alternatives to N-heterocyclic carbenes. They were effective in catalyzing the Stetter reaction, and displayed unique advantages over the commonly used thiazolylidenes and triazolylidenes. They also mediated extended umpolung reactions of enals. In addition, chiral analogues can be accessed readily for applications in enantioselective catalysis.

Synthetic Methods

R. Zhu, S. L. Buchwald* **12655 – 12658**

Enantioselective Functionalization of Radical Intermediates in Redox Catalysis: Copper-Catalyzed Asymmetric Oxytrifluoromethylation of Alkenes

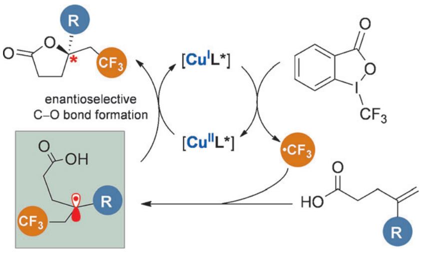

Something radical: An efficient enantioselective oxytrifluoromethylation of alkenes has been developed using a copper catalyst system. Mechanistic studies are consistent with a metal-catalyzed redox radical addition mechanism in which a C–O bond is formed by the copper-mediated enantioselective trapping of a prochiral alkyl radical intermediate derived from the initial trifluoromethyl radical addition.

Hydrogen Storage

Z. Tang, Y. Tan, X. Chen, L. Ouyang,
M. Zhu,* D. Sun, X. Yu* **12659 – 12663**

Immobilization of Aluminum Borohydride Hexammoniate in a Nanoporous Polymer Stabilizer for Enhanced Chemical Hydrogen Storage

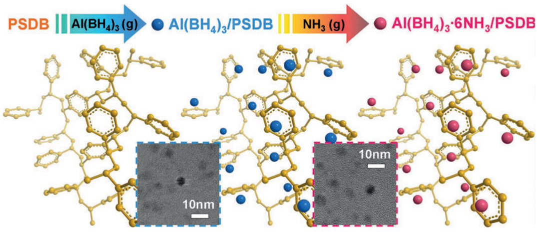

Caught in a trap: The well-distributed $Al(BH_4)_3\cdot 6NH_3$/PSDB (PSDB = poly(styrene-*co*-divinylbenzene)) nanocomposite was synthesized by the stabilization of volatile $Al(BH_4)_3$ within a porous polymer and subsequent treatment with ammonia. This material showed a hydrogen-storage performance that was significantly improved over that of its bulk counterpart. Partial regeneration using hydrazine in ammonia is also described.

Asymmetric Catalysis

X. Xu, P. Y. Zavalij,
M. P. Doyle* ________ **12664 – 12668**

Highly Enantioselective Dearomatizing Formal [3+3] Cycloaddition Reactions of *N*-Acyliminopyridinium Ylides with Electrophilic Enol Carbene Intermediates

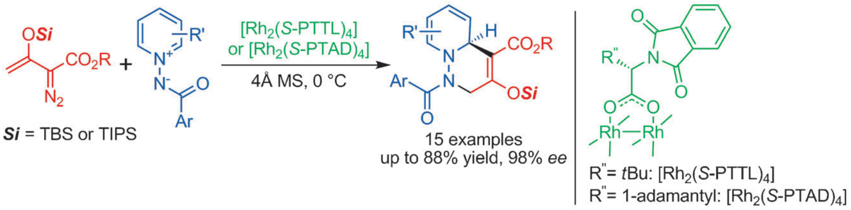

Extrusion of dinitrogen from enol diazoacetates with a Rh^{II} catalyst generates metal enol carbenes. Subsequent vinylogous addition of these to *N*-acyliminopyridinium ylides results in an effective formal [3+3] cycloaddition to give highly substituted 1,2,3,6-tetrahydropyridazines in up to 98 % *ee* and high yield.

Heterocycle Synthesis

U. Sharma, T. Naveen, A. Maji, S. Manna,
D. Maiti* ________ **12669 – 12673**

Palladium-Catalyzed Synthesis of Benzofurans and Coumarins from Phenols and Olefins

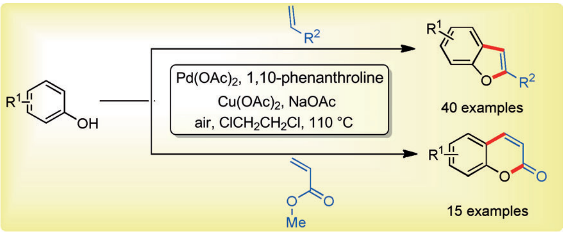

Triple C—H functionalization: Palladium-catalyzed synthesis of benzofurans and coumarins by reacting phenols and unactivated olefins is described. The reaction comprises sequential C—H functionalization and shows diverse functional group compatibility. Preliminary mechanistic studies shed light into the possible mechanisms.

Reductive Bond Cleavage

Y. Ren, M. Yan, J. Wang,* Z. C. Zhang,
K. Yao ________ **12674 – 12678**

Selective Reductive Cleavage of Inert Aryl C—O Bonds by an Iron Catalyst

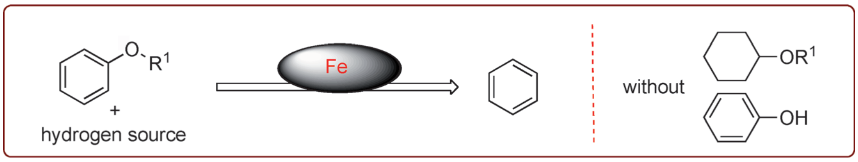

Breaking point: An effective reductive cleavage of inert aryl C—O bonds with an inexpensive iron catalyst has been developed. During this process, the reduction of the arene rings was not observed. This catalytic system also enabled the selective cleavage of the β-O-4 linkage of lignin model compounds under an atmosphere of hydrogen, thus offering an opportunity for the depolymerization of lignin.

Modular Synthesis

E. J. Emmett, B. R. Hayter,
M. C. Willis* ________ **12679 – 12683**

Palladium-Catalyzed Three-Component Diaryl Sulfone Synthesis Exploiting the Sulfur Dioxide Surrogate DABSO

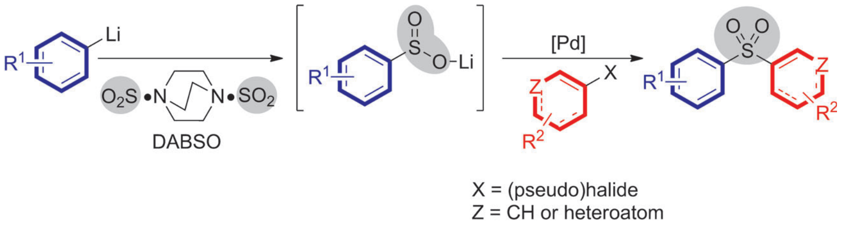

SO(2) efficient: A three-component palladium-catalyzed coupling of aryl lithium compounds; sulfur dioxide (provided by the easy-to-handle solid surrogate, DABSO); and aryl, heteroaryl, and alkenyl (pseudo)halides yields a diverse library of sulfones. An electron-poor XantPhos-type ligand suppresses aryl–aryl exchange and is key to obtaining high yields.

Free-Radical Scavengers

L. Panzella, G. Gentile, G. D'Errico, N. F. Della Vecchia, M. E. Errico, A. Napolitano, C. Carfagna, M. d'Ischia* ____ **12684 – 12687**

Atypical Structural and π-Electron Features of a Melanin Polymer That Lead to Superior Free-Radical-Scavenging Properties

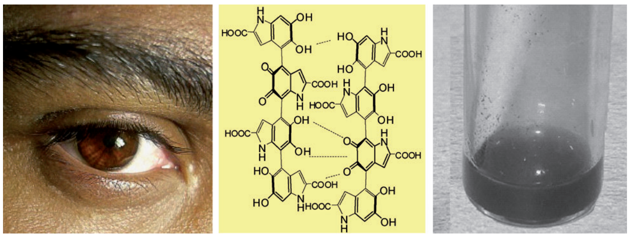

The black we wear: Why nature selected 5,6-dihydroxyindole-2-carboxylic acid (DHICA) to synthesize (photo)protective eumelanin pigments is an enigma. Synthetic DHICA eumelanin has now been shown to be a highly efficient free-radical scavenger in the solid state, which is due to a conformationally interrupted π-electron network associated with atypical optical, paramagnetic, and aggregation properties.

Mechanochemical Activation

S. Immohr, M. Felderhoff, C. Weidenthaler, F. Schüth* ____ **12688 – 12691**

An Orders-of-Magnitude Increase in the Rate of the Solid-Catalyzed CO Oxidation by In Situ Ball Milling

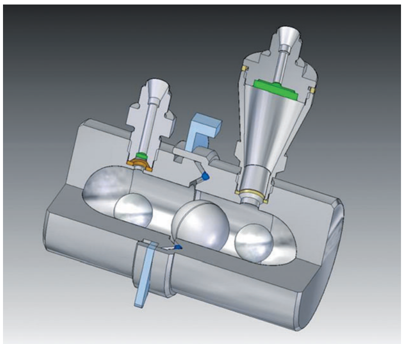

Shaken, not stirred: CO oxidation was carried out continuously in a shaker ball mill. During milling, the reaction rate increases dramatically, but drops rapidly to zero when the mill is stopped. Compared to a conventional experiment in a plug-flow reactor, the rate of a ball-mill reaction catalyzed by Cr_2O_3 is three orders of magnitude higher at room temperature and one order of magnitude higher at 100°C.

Water Splitting

C. Du, X. Yang, M. T. Mayer, H. Hoyt, J. Xie, G. McMahon, G. Bischoping, D. Wang* ____ **12692 – 12695**

Hematite-Based Water Splitting with Low Turn-On Voltages

Power up: The photoelectrochemical performance of hematite in a water-splitting device was improved significantly through surface modification with amorphous $NiFeO_x$ (see graph showing the large cathodic shift observed; FTO = fluorine-doped tin oxide). The measured photovoltage increased from 0.24 to 0.61 V, which yielded a record-low turn-on potential of 0.62 V (versus the reversible hydrogen electrode, RHE).

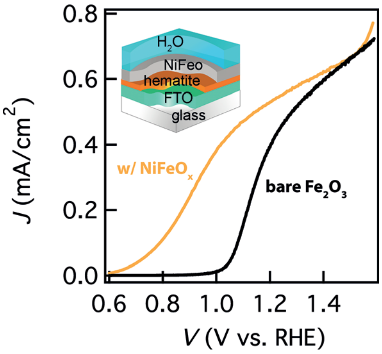

Photochemistry

A. C. Hernandez-Perez, S. K. Collins* ____ **12696 – 12700**

A Visible-Light-Mediated Synthesis of Carbazoles

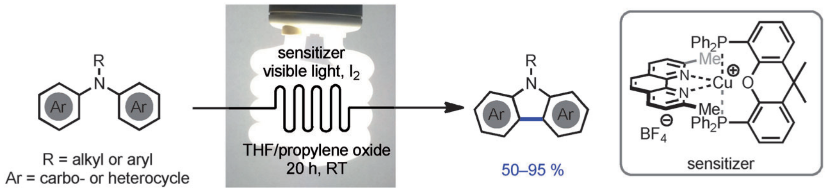

The photosynthetic preparation of *N*-aryl- and *N*-alkyl-bearing carbazoles utilizes continuous flow, visible light, and an in situ formed Cu-based sensitizer (see picture). The method is mild and efficient, and allows the straightforward synthesis of a variety of carbazoles with different substituents, heterocycles, and complex carbon architectures.

Asymmetric Catalysis

S. Goncalves-Contal, L. Gremaud,
A. Alexakis* ______ **12701 – 12704**

Enantioselective Copper-Catalyzed Conjugate Addition of Trimethylaluminium to β,γ-Unsaturated α-Ketoamides: Efficient Access to γ-Methyl-Substituted Carbonyl Compounds

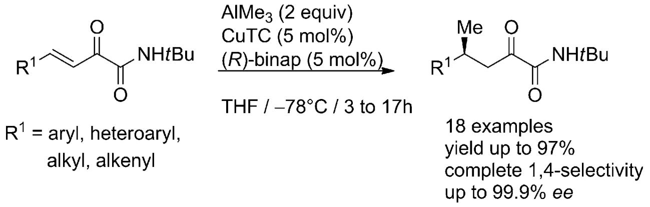

Picture perfect: By using the reagent trimethylaluminium and β,γ-unsaturated α-ketoamides, 1,4-adducts were obtained with perfect 1,4-regioselectivity and good to excellent yields and *ee* values. The potential synthetic utility of the methodology was highlighted by preparation of γ-methyl-substituted carbonyls, key synthons to many natural products. binap = 2,2′-bis(diphenylphosphino)-1,1′-binaphthyl, TC = thiophene carboxylate.

Hydroamination

C. Clavette, J.-F. Vincent Rocan,
A. M. Beauchemin* ______ **12705 – 12708**

Diversity-Oriented Synthesis of Hydrazine-Derived Compounds from Amino Isocyanates Generated In Situ

Behind the mask: Nitrogen-substituted isocyanates are rare and their synthetic potential is virtually untapped. Simple masked precursors can form amphoteric amino isocyanate intermediates in situ, and allows the synthesis of complex hydrazine derivatives upon addition with amines. This reactivity was used in a cascade substitution/hydroamination sequence, and in the assembly of azadipeptide analogues.

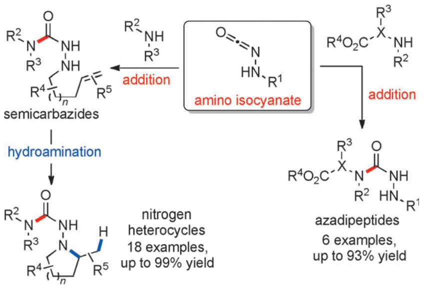

Nanocrystal Sensors

C.-Y. Chiu, M. H. Huang* **12709 – 12713**

Polyhedral Au–Pd Core–Shell Nanocrystals as Highly Spectrally Responsive and Reusable Hydrogen Sensors in Aqueous Solution

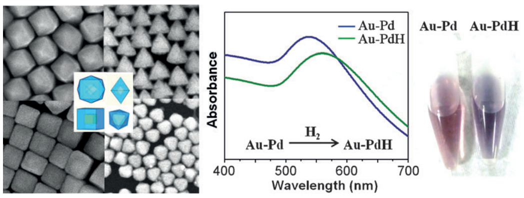

Absorption signals absorption: The surface plasmon resonance absorption band of tetrahexahedral, octahedral, and cubic Au–Pd core–shell nanocrystals with gold nanocrystal cores was strongly red shifted upon hydrogen absorption into the Pd shell. This reversible spectral shift makes the nanocrystals promising recyclable hydrogen-gas sensors. Hydrogen absorption could even be detected visually with smaller core–shell octahedra (see picture).

Organocatalysis

T. Buyck, Q. Wang,
J. Zhu* ______ **12714 – 12718**

Catalytic Enantioselective Michael Addition of α-Aryl-α-Isocyanoacetates to Vinyl Selenone: Synthesis of α,α-Disubstituted α-Amino Acids and (+)- and (−)-Trigonoliimine A

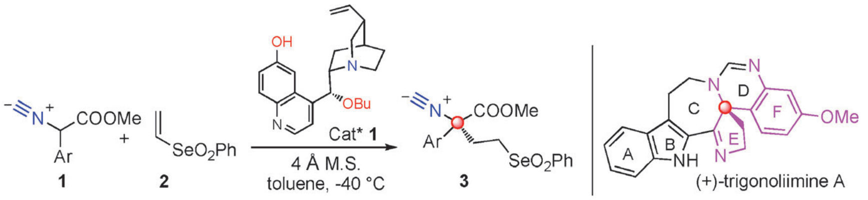

Be like Mike: The title reaction in the presence of the catalyst **1** afforded Michael adducts in excellent yields and enantioselectivities. The adducts were readily converted into α,α′-disubstituted α-amino acids. The enantioselective total synthesis of both (+)- and (−)-trigonoliimine A was accomplished using one of the Michael adducts derived from this methodology. M.S. = molecular sieves.

Cross-Coupling

A. Tsubouchi,* D. Muramatsu,
T. Takeda* ——— 12719–12722

Copper(I)-Catalyzed Alkylation of Aryl- and Alkenylsilanes Activated by Intramolecular Coordination of an Alkoxide

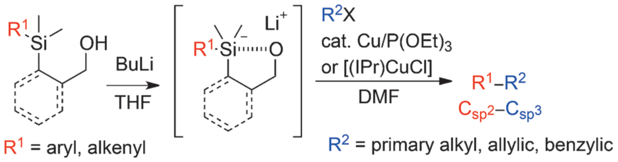

Let's coordinate: Copper(I)-catalyzed cross-coupling of alkenyl- and arylsilanes with primary alkyl iodides as well as allylic and benzylic halides as $C(sp^3)–X$ electrophilic coupling partners has been realized by intramolecular activation through alkoxide coordination. This alkylation tolerates a range of functional groups including a free hydroxy group. IPr = 1,3-bis(2,6-diisopropylphenyl)imidazol-2-ylidene.

Ammonia Synthesis

T. Kandemir, M. E. Schuster, A. Senyshyn,
M. Behrens,* R. Schlögl* 12723–12726

The Haber–Bosch Process Revisited: On the Real Structure and Stability of "Ammonia Iron" under Working Conditions

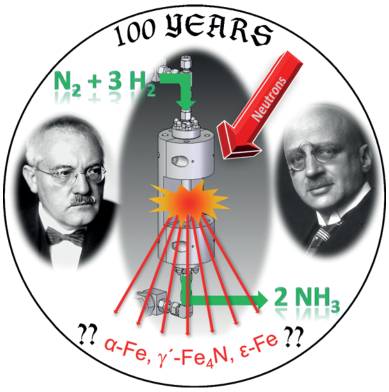

In situ neutron diffraction was used to study the structural properties of an industrial ammonia synthesis catalyst under working conditions similar to those of the Haber–Bosch process. Despite favorable thermodynamics, no indications of reversible bulk nitridation of the iron catalyst was observed in a self-generated ammonia concentration of 12 vol% at 425 °C and 75 bar after 88 h on stream.

Heterocycle Synthesis

K. Graf, C. L. Rühl, M. Rudolph,
F. Rominger,
A. S. K. Hashmi* ——— 12727–12731

Metal-Free Oxidative Cyclization of Alkynyl Aryl Ethers to Benzofuranones

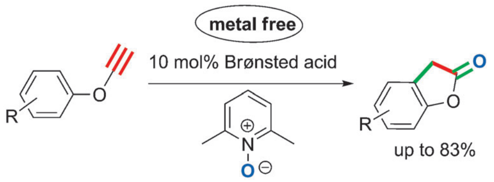

Readily available phenols can be converted into substituted aryl alkynyl ethers, which react with an *N*-oxide as an oxidant and catalytic amounts of a Brønsted acid to provide benzofuranones. If non-terminal alkynyl ethers are applied, a 1,2-hydride shift takes place and phenyl acrylates are obtained. Thus activated alkynes can serve as α-oxy carbene precursors even in the absence of a metal catalyst.

Polyinterhalides

C. Walbaum, M. Richter, U. Sachs,
I. Pantenburg, S. Riedel,* A.-V. Mudring,*
G. Meyer* ——— 12732–12735

Iodine–Iodine Bonding makes Tetra(diiodine)chloride, $[Cl(I_2)_4]^-$, Planar

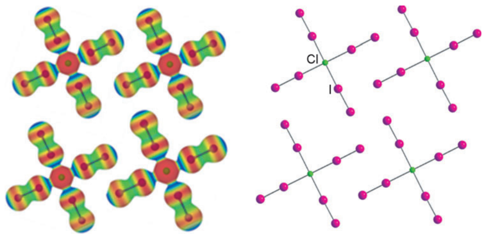

All square: The polyinterhalide $[Cl(I_2)_4]^-$ is square-planar in the crystal structure of $[(H_5O_2)(I_2b15c5)_2][Cl(I_2)_4]$ (I_2b15c5 = diiodobenzo-15-crown-5), although it would be tetrahedral in the gas phase. Along with other effects, such as electrostatic attractions between the cationic and planar anionic layers, iodine–iodine bonding with σ-hole interactions plays a considerable role is stabilizing the square-planar configuration.

β-Peptides

K. V. Kudryavtsev,* P. M. Ivantcova,
A. V. Churakov, S. Wiedmann, B. Luy,
C. Muhle-Goll, N. S. Zefirov,
S. Bräse* ____________ **12736 – 12740**

Alternating Asymmetric Self-Induction in Functionalized Pyrrolidine Oligomers

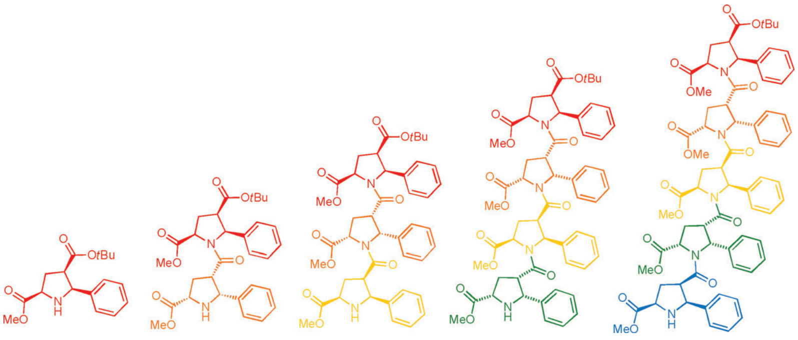

Rainbow of pyrrolidines:
Red, orange, yellow, green, blue (indigo, violet).

Solid-State NMR Spectroscopy

N. Luckgei, A. K. Schütz, L. Bousset,
B. Habenstein, Y. Sourigues,
C. Gardiennet, B. H. Meier,* R. Melki,*
A. Böckmann* ____________ **12741 – 12744**

The Conformation of the Prion Domain of Sup35 p in Isolation and in the Full-Length Protein

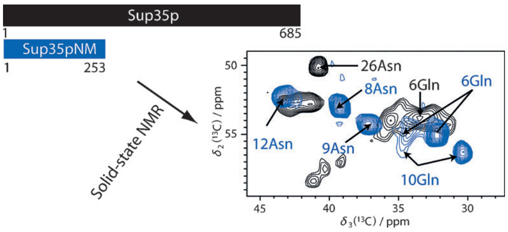

The whole is not the sum of the parts: Fibrils form both from the full-length Sup35 prion protein and also from its isolated NM domain. A conformation analysis of both shows that Sup35NM and fragments thereof, which are often used as convenient models for prion fibril assembly, have a very different conformation of the prion domains.

Supporting information is available on www.angewandte.org (see article for access details).

A video clip is available as Supporting Information on www.angewandte.org (see article for access details).

This article is available online free of charge (Open Access).

This article is accompanied by a cover picture (front or back cover, and inside or outside).

The Very Important Papers, marked VIP, have been rated unanimously as very important by the referees.

The Hot Papers are articles that the Editors have chosen on the basis of the referee reports to be of particular importance for an intensely studied area of research.